Diagnosis of Leptomeningeal Metastases Disease in MRI Images by Using Image Enhancement Methods

Mehmet Gül[1], Sadık Kara[1], Abdurrahman Işıkdoğan[2], and Yusuf Yarar[3]
[1]Biomedical Engineering Institute, Fatih University, Istanbul
[2]Hospital of Oncology, Dicle University, Diyarbakır
[3]Selahaddin'i Eyyubi Hospital, Diyarbakır

Abstract: *Leptomeningeal Metastases (LM) disease is the advanced stages of some complicated cancers. It contaminates in the Cerebrospinal Fluid (CSF). Tumors might be in macroscopic or microscopic sizes. The medical operation is more risky than other cancers. Consequently, diagnosis of leptomeningeal metastases is important. Different methods are used to diagnose LM disease such as CSF examination and imaging systems Magnetic Resonance Imaging (MRI) or Computer Tomography (CT) examination. CSF examination result is more accurate compared to CT or MRI imaging systems. However imaging systems' results are taken more early than CSF examination. Some details in MRI images are hidden and if the proper image enhancement method is used, the details will be revealed. Diagnosis of LM disease can be earlier with accurate results at that time. In this study, some image enhancement methods were used. The probability of result of Logarithmic Transformation (LT) method and Power-Law Transformation (PLT) method were almost the same and result was p=0.000 (p<0.001), and statistically high result was obtained. The probability of Contrast Stretching (CS) method was p=0.031 (p<0.05), and this result was statistically significant. The other four methods' results were insignificant. These methods are Image Negatives Transformation (INT) method, thresholding transformations method; Gray-Level Slicing (GLS) method and Bit-Plane Slicing (BPS) method.*

Keywords: *Cerebrospinal Fluid (CSF) examination, Computed Tomography (CT), Image Enhancement methods, Leptomeningeal Metastases, Magnetic Resonance Imaging (MRI).*

Received March 23, 2015; accepted August 12, 2015

1. Introduction

The meninges layer consists of three layers and surrounds all around the brain and spinal cord. Furthermore, meninges layer protects brain and spinal cord. Cerebrospinal fluid stream and blood stream occur in that layer. The meninges layer composes of dura mater, arachnoid mater and pia mater. Dura mater is outermost layer, closest to the skull and the thickest layer. Arachnoid mater is the middle layer filled with liquid and web-like structure. Nutrients needed by the brain and waste materials are exchanged with capillaries located in this structure. Pia mater is innermost layer and most fragile layer. Capillaries located in the arachnoid mater convert pia mater into a porous structure. Pia and arachnoid layers seem to be a component of a two-layer structure and are called pia-arachnoid layer or leptomeninges layer.

Some types of complicated cancer in advanced stages contaminate to leptomeningeal layer. Central Nervous System (CNS) tumors such as medulloblastoma or ependymoma tumors disseminate within craniospinal leptomeningeal layer axis. This situation is observed between 10% and 30% cancer patients [3]. Cancer cells disseminate throughout the spinal fluid by blood or by CerebroSpinal Fluid (CSF). The invasion of cancer cells are defined as Leptomeningeal Metastases (LM) also known as Carcinomatous Meningitis (CM) [18, 26]. LM tumors are formed macroscopic or microscopic at autopsy of cancer patients. Dissemination is frequently emerging in clinical oncology because of chemotherapy or other medical procedure. These medical operations are failure of penetration the blood-brain, the blood-CSF and brain-CSF barriers [3, 10].

LM's solid tumors are seen as an advanced level of systemic disease and usually appear as parenchymal brain metastases [36]. After the diagnosis of the primary tumor, brain metastasis is detected. Diagnosis of the primary tumor with symptoms of the disease at the same time can be very rare [8]. Symptoms in 67% of patients are brain metastasis [28]. Leptomeningeal metastasis is diagnosed with imaging systems such as Computer Tomography (CT) and asymptomatic Magnetic Resonance Imaging (MRI). The study conducted between 1973 and 1993 was regarding symptoms of LM patients. In the study, the data was obtained from 10% of the patients. The symptoms were headache between 24% and 53%, focal weakness between 16% and 40%, altered mental status between

24% and 31%, seizures between 15% and 16%, and ataxia between 9% and 20% [27, 35]. In another study, conducted in 2010, with about 60,000 of 70,000 results observed in cancer patients and LM disease was observed 16% of patients with lung cancer, 10% of patients with renal cell cancer, 7% of patients with melanoma, and in 1% of patients with colorectal carcinoma [17, 31].

Advances in diagnostic methods have been investigated for LM disease up till now. Even more complicated biomarkers have been intended to facilitate diagnosis. For instance, some antigens such as tumor antigen as well as the enzymatic activity of β-glucuronidase were detected in the CSF of brain in 1980. Unfortunately, up to now no other antigen has been detected in any other antigens. According to this obtained antigen, today, the detection of neoplastic meningitis has become easier. Thus, the diagnosis of patients is usually adhered to the process of Cytology and the clinical effect. If any abnormality is found in cranial nerve, the sample of the blood-brain by penetration is checked by pathologist [32]. The cell counts, protein, opening pressure and glucose value are checked in CSF measurement. CSF is carried out with the help of a long needle and the liquid obtained should be in the range of 10 to 20 ml. Before this operation, an anesthetic spray is applied to the skin. On the other hand, many people dominate by the fear of the possibility of being paralyzed. Such a possibility is one in a millions.

CSF fluid intake is usually carried out by specialists and is rarely encountered in a negative situation. During process, respectively, the theoretical risks of CSF are listed as infection, local bleeding, nerve injury and brain herniation. Dizziness may occur after the procedure. This is due to leakage of cerebrospinal fluid [12]. Cytology of CSF plays an important role for the diagnosis of LM disease. However, in the study of Patchell et al. conducted on 54 patients who need biopsy, 11% of patients was with glial tumor biopsy, no result has been achieved, including abscess [4]. CSF cytology test repetition may result in increased sensitivity of diagnosis, the positive result is usually emerges in spread of tumor and as a sign of a deteriorating situation [29].

Early diagnosis and management of complications of this disease are often difficult, and possess a major problem. Thus, modern treatment techniques are used for early diagnosis, the treatment is started early by obtained data and in this way the patients' life expectancy would be prolonged. Although cytology results are more accurate results, the results are obtained in a shorter time with imaging system imaging system is preferred at first. If there is still suspected metastases, biopsy should be considered in option by physicians. MRI imaging modalities are especially used cancer diagnosis. MRI imaging system gives more successful than CT imaging system for identifying lesion distribution and numbers or size of lesions [4, 9]. MRI gets image by the movement and the density of hydrogen atoms of the soft tissue [6]. Therefore, the referenced MRI method is one of the first methods to diagnose occurrence of LM disease [3, 10].

In this study, image processing methods are used to detect spread cancer cells on the surface of leptomeningeal layer. Despite the advantages of MRI imaging system, diagnosis of LM disease with a complex structure cannot give accurate results all the time. The spreading cancer cells, the distribution and the size of lesions are observed clearly in cytology cases than MRI imaging system. The aim of the study is to obtain more precise results from MRI imaging system with using image processing method to diagnose LM cancer.

2. Database Used

In the study, the data was obtained over the last decade which the data of patients admitted to the hospital at different times. It has been examined data for more than a thousand cancer patients admitted to the hospital and only forty-two leptomeningeal metastases patients was able to find through these. The records obtained from radiology services of two state hospitals. So that the small number of patients due to the very low occurrence of the leptomeningeal metastases.

Patients admitted to several clinics were followed with the diagnosis of malignant tumors. These patients were given precise diagnosis with pathologically. Patients' images which were discussed were taken radiology clinics and in MRI request form leptomeningeal metastases pre-diagnosed patients were included.

In the study, forty-two patients were dealt with and eighteen of these patients were men, twenty-four of these patients were women and average age 43.67 (± 19.43) shown in Table 1. MRI examinations of all patients were followed and all of the sequences of these patients and contrast-enhanced images were included (used MRI sequences; T1 axial, coronal, sagittal, T2 axial, coronal, Flair axial, sagittal and contrast-enhanced T1 axial, coronal and sagittal images). Whether MRI sequences that were missing or images which were difficult to assess due to patients motion were not included. MRI imaging system with 1.5 tesla property was used.

Table 1. Demographic Table of This Study.

	Number (%)	**Mean age ± standard deviation**
Male	18 (42.9)	44.11 (± 18.471)
Female	24 (57.1)	43.33 (± 20.506)
Sum	42 (100)	43.67 (± 19.429)

In our study, we used Magnetic Resonance Imaging as imaging modality. T1 and T2 weighted scanning mode are preferable to highlight the Cerebrospinal Fluid [37]. Axial MRI images are used to eliminate non-brain tissues such as mouth, skull jawbone. Concerning axial MRI images, LM disease marks become invisible in non-brain especially mouth, jawbone, and skull. Because of this reason, the uppermost and undermost images among axial scans include such non-brain organs as jawbones are not examined.

3. Used Methods

Imaging systems are the first method of diagnosis of cancer patients. The aim of this study is to facilitate diagnosis of cancer cases which are increasing with each passing day now. If there is still a suspected cases of the results obtained by imaging methods, the piece of tissue taken from patients is sent to pathology or CSF measurement method is applied for the diagnosis of cases. Radiologists cannot always define LM disease by MRI images, therefore, this situation causes a difficult problem with diagnosis of LM. If resolution of images is increased or image improvement is done with image enhancement methods, radiologists are able to define easily malignant tumors on the MRI images.

3.1. Logarithmic transformation:

This method reveals the hidden details in rich image. LT method reduces some variables value on the image and increases the others. The dark pixels replace with brightness pixels. The brightness pixels are obtained with LT method. Thus, the details hidden in the dark side of the image are revealed by the LT method. Logarithmic transformation corresponds with gamma transformation (gamma<1). Furthermore, image sharpening and contrast stretching applications are held together with this method. Logarithmic transformation formulas is:

$$G = c * log(1 + |r|) \tag{1}$$

Where c is constant and it is assumed that $r \geq 0$ [20]. Brightness pixels on the image are obtained by higher "c" value (1). LT method enhances dynamic ranges of hidden pixels and increases the visibility of the pixels.

The dynamic range of low gray-level values of the input image are expanded by LT methods. On the other hand, the dynamic range of images with large variations in pixel values are compressed by this method. In Figure 1, LT method exceeds the dynamic range of image in the capability of the display device [5, 14].

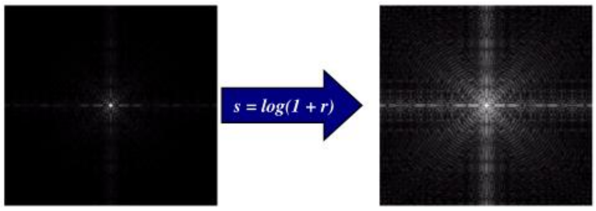

a) It is gotten by range between 0 and 1.5 x 106.

b) Result obtained by performing logarithmic transformation (c = 1 and range between 0 and 6.2).

Figure 1. Effects of logarithmic transformation on Fourier Spectrum image.

Reverse process of logarithmic transformation is called Inverse Logarithmic Transformation (ILT). The dark pixels value are extracting and the bright pixel values are compressed [16, 23]. Logarithmic and inverse transformations, especially, are used for the high and low pixel values of images. In Figure 2 shows the significant differences of Fourier spectrum image and rendered Fourier images by logarithmic transformation [13, 22].

3.2. Power-law transformation:

This method is known as gamma correction method. The hidden details in the images are obtained with different ɣ coefficients. Different monitors demonstrate images with different intensity and clarity levels. The reason is that each monitors perform gamma correction in certain ranges. A good monitor attempts to display all the images in the best contrast and the best solution to user. Effects of Power-Law Transformation (PLT) method of images is formulated with:

$$s = cr^{\gamma} \tag{2}$$

Effects of PLT method of images are proportional to c and ɣ values (2). Contrast of images and sharpness of images do not have any influence on PLT method [1, 22]. Fractional values of ɣ map a narrow range of dark input values into a wider range of output values, on the other hand, they map a wider range of output values into a narrow range of dark input values [11, 19].

PLT method changes the brightness as well as the ratios of R to G to B. According to this method, fracture can be more visible and PLT method enhances the background.

3.3. Contrast stretching:

This method is one of the basic piecewise liner function. If the number of dark pixels on images are more than others, the hidden details must be revealed on images remaining on dark parts. The brightness of dark sides in images must be increased to uncover the hidden details. Contrast Stretching (CS) method is one of the way of increasing the brightness of the dark dynamic pixels. This method increases the brightness of dark dynamic pixel value on images and by this way, the brightness of image is improved [20, 22].

In Figures 2-a, 2-b, 2-c, 2-d, there is a pollen image magnified about 700 times with electron microscope.

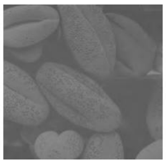

a) An 8-bit image with density of dark pixels.

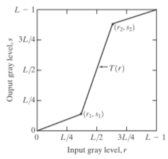

b) Control points are defined with the CS method.

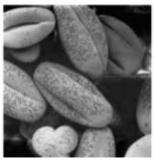

c) The first image is obtained with the first control point of the CS method.

d) The last image is obtained with the second point of the CS method.

Figure 2. Effects of contrast stretching method on 8-bit image of pollen.

The brightness of this image has been enhanced by the CS method, and the control points of r_1, s_1 and r_2, s_2 are determined for this process. The shape of the transformation function is controlled by the locations of points (r_1, s_1) and (r_2, s_2) [11, 19]. Gray levels does not changes when location point r_1 is equal to s_1 and r_2 is equal to s_2. Otherwise, location point r_1 is equal to r_2 and s_1=0 and s_2=L-1, the transformation becomes a thresholding function, and a binary image is obtained. The necessary contrasted changes on the image are performed with a medium of (r_1, s_1) and (r_2, s_2), and the brightness results are obtained. Usually, $r_1 \leq r_2$ and $s_1 \leq s_2$ are accepted [20, 25].

3.4. Image Negative Transformation:

This method is the simplest image enhancement method, and it creates the opposite of the original image. The main aim of this image enhancement is to expand the white or the gray details embedded in the dark areas on the image, as shown in Figure 3. Although a small lesion in the original mammogram image is displayed and the amount of total tissue in both images is equal, the analysis of the negative image is easier than that of the first image. The image negative has gray levels in the range of "0, *L*-1".

$$s = L\text{-}1\text{-}r \qquad (3)$$

The image negative is obtained by the equation below. The format of the processed image is 8-bit, and extractions of each pixel's value are worth 255. MxN variables are in the image, in which M is the line and N is the column, the image is defined as l(*m*, *n*), and the negative image is defined as *g*(*m*, *n*) based on *f*(*m*, *n*); the equation is the following.

$$g(m,n) = 255 - f(m,n) \begin{cases} 0 \leq m < M \\ 0 \leq n < N \end{cases} \qquad (4)$$

Eliciting details in the following mammography image is demonstrated with image negative transformation.

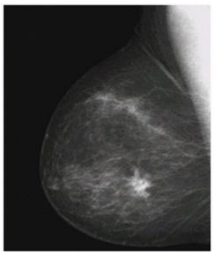

a) The original image of the human breast with mammography.

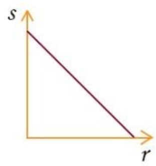

b) The obtained processed image with the image negative transformation.

Figure 3. Effects of Image Negative Transformation on image of the human breast with mammography.

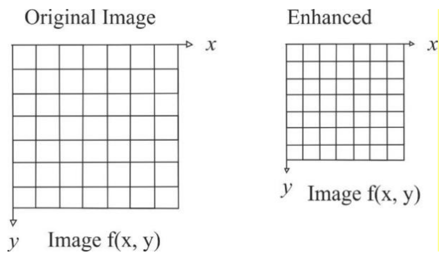

$$s = intensity_{max} - r \qquad (5)$$

This example shows how the human breast analysis with image negative transformation is easier [21].

3.5. Thresholding Transformation

This method gives effective results that distinguish different density or colored tissues from the background in the image.

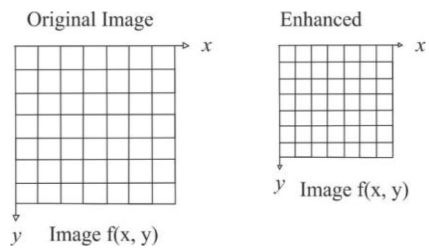

$$s = \begin{cases} 1.0 r > threshold \\ 0.0 r \leq threshold \end{cases} \qquad (6)$$

The image to be processed having bright colors on a dark background is defined as one-dimensional. The input of the thresholding operations generally prefers a color image or grayscale. Dark pixels symbolize the background, light-colored or white pixels symbolize tissue, or vice versa. Implementations are basically determined by the threshold parameters. Before the image is put into practice, the threshold of each pixel in the image is determined. If the pixel density is greater than the threshold value, the pixels are assigned the white value; if it is lower, they are assigned the black value [5, 15].

3.6. Gray-Level Slicing:

This method is an image enhancement method for persons engaged in images contained in a certain range of [A………B]. It is always intended to elicit something in a given tissue. For example, the desired image is revealed by neglecting unwanted water stains on X-ray images from satellite imagery.

a) [A, B] of the gray levels and reduces all others to a constant level.

b) Highlights range [A, B] but preserves all other levels.

c) An image.

d) Result of using the transformation.

Figure 4. Effects of gray level slicing on image.

There are many methods of carrying out division on an image, and these methods are divided into two categories. In the first, the high gray values in the image are put forward, and the remaining values are reduced. In the second, the brightness of the desired range of gray tones is increased, while the background and the other gray tones are protected. The first approach is illustrated in the "c" shape, while the second is illustrated in the "d" shape shown as an example [20].

3.7. Bit-Plane Slicing

This method impacts the entire image. Pixels of images are composed of digital numbers, so the image can be defined as a sequence of numbers of bits. Each image is formed from layers, as in the following figure. The format of a processed image lets it be accepted as 8-bits. In this case, the form of the image parts is considered in 1 bit, and the bit-planes are ranked from 0 to 7. Delamination of an 8-bit image is represented in Figure 5.

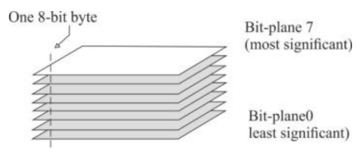

Figure 5. Delamination of an image.

Figures 6 and 7 show an 8-bit fractal image. The fractal image is derived from a mathematical equation, and it is a multi-layered image. The higher-order bits in the image contain the important information of the visualization of the image. The remaining bit layers on the image give a harmonic alignment. The resulting fractal image segmentation helps image analysis [20].

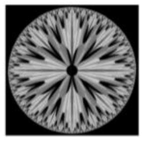

Figure 6. An 8-bit fractal image. (A fractal is an image generated from mathematical expressions). (Courtesy of Ms. Melissa D. Binde, Swarthmore College, Swarthmore, PA).

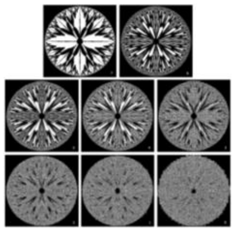

Figure 7. The 8-bit planes of the image in figure 6. The number at the bottom-right of each image identifies the bit plane.

4. Results

The MRI images of the leptomeningeal metastases cancer patients admitted to the hospital on different dates were examined. The sequences of all patients discussed were full. Images were obtained with 1.5 tesla capable devices. The spinal fluid of some of the LM patients was taken and sent to pathology. The exact results of the samples sent to pathology could not be obtained in all cases. The CSF examination is almost certainly a reference by a doctor.

LM patients' MRI images discussed were examined to overcome the disadvantage situations mentioned above. Images were analyzed using the different image enhancement methods and the results were compared with each other. MRI images are rich content and some details are hidden in the dark side of images. These hidden details were examined separately with some different methods. These methods were LT method, PLT method, CS method, INT method, thresholding method, GLS method and BPS method.

The MRI images were examined to overcome the disadvantageous situations mentioned above. Images were analysed using different image enhancement methods, and the results were compared with each other. MRI images are rich in content, but some details are hidden in the dark side of the images. These hidden details were examined separately using different methods. These methods were the LT method, PLT method, CS method, INT method, thresholding method, GLS method and BPS method.

Before applying image enhancement methods, clinically forty-two patients were suspected and sixteen of these patients were diagnosed with LM disease by contrast-enhanced MRI images. However, forty patients were diagnosed as metastases after applying two image enhancement methods, LT and PLT methods.

PLT method is known gamma correction and also LT method corresponds with gamma correction (gamma<1). The common point of these two methods are to reveal the hidden details in dark area. It is used in brain MRI images and tumour areas are revealed.

The tumour areas cannot be selected in raw brain MRI images. After image enhancement processing, the main purpose is that use power law transformation and logarithmic transformation for segmentation of medical images improving the accuracy and exactness [30].

PLT and LT methods are important to display an image accurately on a monitor because of using gamma correction parameter. The changing of gamma parameter of monitor not only effects brightness, but also effects the ratios of red-to-green-to-blue.

The results obtained with two different methods were applied in chi-square test and the success probability was P=0,000000005 (P<0,001). The obtained results are represented a very high statically success shown in Table 2 and sample of processed images are shown in Figure 8.

Table 2. the Statistical Results of LT Method, PLT Method and CS Method and Comparison of Results of Obtained by Three Methods.

	Diagnosis of LM disease with LT and PLT methods		**Diagnosis of LM disease with CS method**		**Comparison of three methods**
Numbers of patients	Defined	Non-defined	Defined	Non-defined	0.000 (< 0.001)
	40	2	22	20	
p-value	0.000 (< 0.001)		0.031 (< 0.05)		

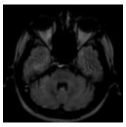

a) Raw MRI images.

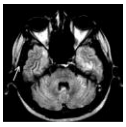

b) Enhanced by Contrast Stretching method

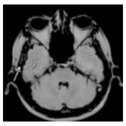

c) Enhanced by LT method.

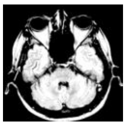

d) Enhanced by PLT method.

Figure 8. One of image in the study enhanced with three different methods.

The initial clinical assessment of leptomeningeal metastases patients are shown in Table 3. Furthermore, the diagnosis of leptomeningeal metastases with raw MRI images are shown and the success rates after applied image enhancement processes-LT and PLT methods are shown.

Table 3. Results of image enhanced with lt and plt methods (all-acute lymphoblastic leukemia).

Cancer type		**LM diagnosis before image process**		**Total**	**LM diagnosis after LT and PLT methods image process**		**Total**
		Exists	**Non-exists**		**Exists**	**Non-exists**	
All*	**Count**	3	10	13	11	2	13
	%	18.8 %	38.5 %	31 %	27.5 %	100 %	31 %
Lung cancer	**Count**	4	9	13	13	0	13
	%	25 %	34.6 %	31 %	32.5 %	0 %	31 %
Breast cancer	**Count**	8	3	11	11	0	11
	%	50 %	11.5 %	26.2 %	27.5 %	0 %	26.2 %
Gastric cancer	**Count**	1	1	2	2	0	2
	%	6.3 %	3.8 %	4.8 %	5 %	0 %	4 %
Other cancer	**Count**	0	3	3	3	0	3
	%	0 %	11.5 %	7.1 %	7.5 %	0 %	7.1 %
Total	**Count**	16	26	42	40	2	42
	%	100 %	100 %	100 %	100 %	100 %	100 %

The success rates of CS method applied to raw MRI images are shown in Table 4. These LM patients MRI images were examined by CS method and twenty-two patients were diagnosed to LM disease after image processing. The obtained result was applied in McNemar test and the success probability was defined as P=0,031 (p<0,05). The result was statistically significant.

Table 4. Results of image enhanced with CS method.

Cancer type		**LM before image process**		**Total**	**LM after CS method image process**		**Total**
		Exists	**Non-exists**		**Exists**	**Non-exists**	
All	**Count**	3	10	13	5	8	13
	%	18.8 %	38.5 %	31 %	22.7 %	40 %	31 %
Lung CA	**Count**	4	9	13	7	6	13
	%	25 %	34.6 %	31 %	31.8 %	30 %	31 %
Breast CA	**Count**	8	3	11	8	3	11
	%	50 %	11.5 %	26.2 %	36.4 %	15 %	26.2 %
Gastric CA	**Count**	1	1	2	2	0	2
	%	6.3 %	3.8 %	4.8 %	9.1 %	0 %	4 %
Other CA	**Count**	0	3	3	0	3	3
	%	0 %	11.5 %	7.1 %	0 %	15 %	7.1 %
Total	**Count**	16	26	42	22	20	42
	%	100 %	100 %	100 %	100 %	100 %	100 %

The results obtained from INT method were not sufficient. There were only four patients diagnosed to LM disease, the other patients were not diagnosed. The statistical value of INT method is 0,571. This value is obtained with Chi-Square test. It was insufficient statistical results (p > 0,05). This statistical value was even lower than the evaluations of raw MRI images.

Contrast stretching method is one of the simpler piecewise linear function and it tries to extend the narrow range of image pixel values over a wider range. On the other hand, illumination of CS method is poorer than PLT and LT methods. In addition to this, lack of dynamic range of CS method in imaging sensor can produce low-contrast images. Because of this, the accuracy of CS method is not good at PLT and LT methods [24].

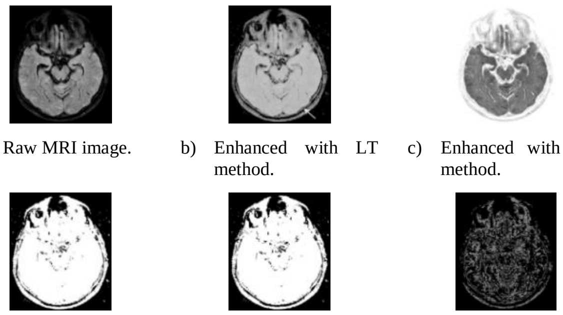

a) Raw MRI image. b) Enhanced with LT method. c) Enhanced with INT method.

d) Enhanced thresholding method. e) Enhanced with GLS method. f) Enhanced with BPS method.

Figure 9. Effects of five different image enhanced methods on the same raw image.

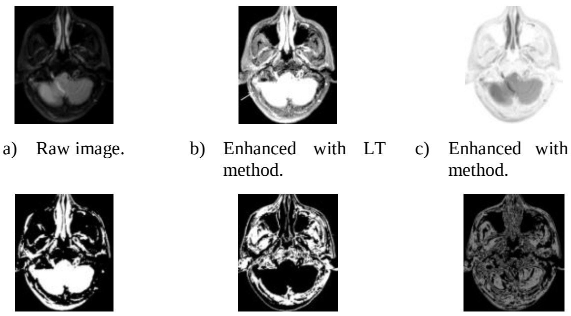

a) Raw image. b) Enhanced with LT method. c) Enhanced with INT method.

d) Enhanced thresholding method. e) Enhanced with GLS method. f) Enhanced with BPS method.

Figure 10. Effects of five different image enhanced methods on the same raw image.

The evaluations of the raw MRI images were more successful than the evaluation of INT method, GLS method, Thresholding method and BPS method as shown in Figures 9 and 10. The results of logarithmic transformation and power-law transformation methods were almost the same. The results of these methods were compared with each other and the probability was P=0,000 (p<0,001) (Table 2). This final result was obtained Cochran test and the result was represented a very high statically success.

5. Discussions

Contrast-enhanced images are obtained by injecting the drug to the patient and compared to non-contrast-enhanced images, flair images, help obtaining detailed images; however, suspected metastases cases on contrast-enhanced images cannot be even realized.

MRI imaging system is a method to emerge brain tumors. MRI method is the first preferred method, the reason is to consume less time than other procedures. As it is known, CSF analysis gives more successful result compared to MRI imaging system. In order to increase the sensitivity of MRI imaging system, many different studies are carried out. The studies mainly focus on MRI imaging system, such as increasing the strength of tesla, the amount of the substances used to obtain contrast-enhanced images and etc.

Demonstration of LM tumors with MRI imaging system gives more accurate results than CT imaging system [7, 33, 34]. Standard contrast-enhanced MRI images are obtained by gadolinium injection in patients. Gadolinium (Gd) enhanced MRI is to detect LM disease. Gd-MRI images were not sensitive enough in many studies. Detection of LM disease with Gd-MRI images is 34% to 71% ratio. The main objective of some studies carried out is to increase the sensitivity of Gd-MRI images, such as the amount of magnetization saturation injected, using combination of all sequences of MRI images and etc., [38].

Contrast-enhanced MRI images offer more details compared with Flair MRI images. The ratio of exposing LM disease with the standard contrast-enhanced MRI images is low, thus it is difficult to diagnose. The studies using image enhancement methods to expose LM tumors in MRI images are negligible. The scope of study was applied image enhancement methods to Flair and contrast-enhanced MRI images and statistically higher accuracy was obtained.

6. Conclusions

Forty-two patients' contrast-enhanced MRI images were taken in the hospital radiology services and these patients were followed up malignant tumors in the clinical. However, this disease is a rare type of cancer and the definitive diagnosis through MRI images provide also a difficult situation as much. The different image enhancement methods were applied to LM patients' MRI images and the successful results were obtained. Especially, highly successful results were obtained by logarithmic transformation method and power-law transformation method. The statistically significant result was obtained by contrast stretching method.

Advanced studies were investigated and radiologists diagnosed LM tumors by investigating raw-MRI images. Diagnosis of LM disease on MRI images with image enhancement methods has not been applied up till now.

The major conclusion of this study is that if LM patients MRI images' gamma range changes in certain range, LM tumors will be revealed more clearly. The results obtained by LT method and PLT method have been more successful than results of CS method. The statistically high successful results have obtained in this study to reveal tumors of leptomeningeal metastases. However, especially the success of LT method and PLT method to reveal LM tumors can be generalized further by increasing the number of cases.

References

[1] Bankman I., "Handbook of Medical Image Processing and Analysis", *Academic Press*, 2008.

[2] Boehm B., A "Spiral Model of Software Development and Enhancement", *IEEE Computers*, vol. 21, no. 5, pp. 61-72, 1988.

[3] Bomgaars L., Chamberlain M., Poplack D., Blaney S., "Leptomeningeal Metastases*", Oxford University Press*, 2002.

[4] Brooks H., Christian A., May A., "Pregnancy, Anaesthesia and Guillain Barre Syndrome", *Anaesthesia Journal*, vol. 55, no. 9, pp. 894-898, 2000.

[5] Castleman K., "Digital Image Processing", *Prentice-Hall*, 1996.

[6] Chamberlain M., "Neoplastic Meningitis: a Guide to Diagnosis and Treatment", *Current Opinion in Neurology Journal*, vol. 13, no. 6, pp. 641-649, 2000

[7] Chamberlain M., Sandy A., Press G., "Leptomeningeal metastasis: a comparison of gadolinium-enhanced MR and contrast-enhanced CT of the brain Neurology", *Neurology* vol. 40, no. 3, pp. 435-438, 1990.

[8] Chambers P., Davis R., Blanding J., and Buck F., "Metastases to Primary Intracranial Meningiomas and Neurilemmomas", *Arch Pathol Lab med*, vol. 104, no. 7, pp. 350-354, 1980.

[9] Damodharan S. and Raghavan D., "Combining Tissue Segmentation and Neural Network for Brain Tumor Detection", *The International Arab Journal of Information Technology*, vol. 12, no. 1, pp. 42-52, 2015.

[10] Drappatz J. and Batchelor T., "Leptomeningeal Metastasis", *American Society of Clinical Oncology Educational Book*, 2009.

[11] Ertürk S., "Digital Image Processing", *National Instruments Corporation*, 2003.

[12] Freilich R. and Krol G., DeAngelis L., "Neuroimaging and Cerebrospinal fluid Cytology in the Diagnosis of Leptomeningeal Metastasis", *Annals of Neurology*, vol. 38, no. 1, pp. 51-57, 1995.

[13] Gonzalez R., Woods R., "Digital Image Processing using MATLAB", *Prentice Hall*, 2008.

[14] Jähne B., "Digital Image Processing", *Springer*. ISBN 3-540-67754-2.

[15] Jain A., "Fundamentals of Digital Image Processing", *Prentice Hall*, 1989.

[16] Jain R., Kasturi R., Schunck B., "Machine Vision", *McGraw-Hill International Edition*, 1995.

[17] Jemal A., Siegel R., Xu J., and Ward E., "Cancer Statistics," *Cancer Journal for Clinicians*, vol. 60, no. 5, pp. 277-300, 2010.

[18] Lee A., Wallace C., Rewcastle B., and Sutherland G., "Metastases to Meningioma," *American Journal of Neuroradiology*, vol. 19, no. 6, pp. 1120-1122, 1998.

[19] Lim J., "Two-dimensional Signal and Image Processing", *Prentice Hall*, 1990.

[20] Lothar S., Anja T., Per S., Roland O., Ralph B., Gerhard W., Alaleh R., "Fully Automatic Detection of Deep White Matter T1 Hypointense Lesions in Multiple Sclerosis," *Physics in Medicine and Biology*, vol. 58, no. 23, pp. 8323-8337, 2013.

[21] Maini R., Aggarwal H., "A Comprehensive Review of Image Enhancement Techniques," *Journal of Computing*, vol. 2, no. 3, pp. 8-13, 2010.

[22] Marques O., "Practical Image and Video Processing Using MATLAB", *IEEE Press*, 2011.

[23] McAndrew A., "An Introduction to Digital Image Processing with Matlab", *Course Technology Press Boston*, MA, United States ISBN:0534400116, 2004

[24] Mohanapriya N., Kalaavathi B., "Medical Image Enhancement Using Adaptive Wiener Filter and Contrast Stretching Techniques," *Australian Journal of Basic and Applied Sciences*, vol. 9, no. 10, pp. 154-160, 2015.

[25] Nixon M., Aguado A., "Feature Extraction and Image Processing", *Oxford: Academic Press*, 2008.

[26] Norden A.D., Wen P.W., Kesari S., "Brain Metastases", *Current Opinion in Neurology*, 18:654–661, 2005

[27] Nussbaum E., Djalilian H., Cho K., and Hall W., "Brain Metastases. Histology, Multiplicity, Surgery, and Survival," *Cancer*, vol. 78, no. 8, pp. 1781-1788, 1996.

[28] Omar A., Mason W., "Neurologic Complications of Cancer", *Oxford University Press*, 2009.

[29] Patchell R., Tibbs P., Walsh J., Dempsey R., Maruyama Y., Kryscio R., Markesbery W., Macdonald J., and Young B., "A Randomized Trial of Surgery in the Treatment of Single Metastases to the Brain," *The New England Journal of Medicine*, vol. 322, no. 8, pp. 494-500, 1990.

[30] Roy S. and Bandyopadhyay S., "Automated computer aided diagnosis system for brain abnormality detection and analysis from MRI of brain," *International Journal of Advances in Computer Science and Technology*, vol. 4, no. 3, pp. 10-17, 2015.

[31] Schellinger P.D., Meinck H.M., and Thron A., "Diagnostic Accuracy of MRI Compared to CCT in Patients with Brain Metastases," *J Neurooncol*. 44(3):275-81, 1999

[32] Schold S.C., Wasserstrom W.R., Fleisher M., Schwartz M.K., Posner J.B., "Cerebrospinal Fluid Biochemical Markers of Central Nervous System Metastases" *Ann Neurol*. Dec;8(6):597-604. 1980

[33] Schumacher M., Orszagh M., "Imaging Techniques in Neoplastic Meningiosis," *Journal*

of Neuro-Oncology, vol. 38, no. 2, pp. 111-120, 1998.

[34] Sze G., Soletsky S., Bronen R., Krol G., "MR Imaging of the Cranial Meninges with Emphasis on Contrast Enhancement and Meningeal Carcinomatosis," *AJNR Am J Neuroradiol*., vol. 153, no. 5, pp. 1039-1049, 1989.

[35] Tosoni A., Ermani M., Brandes A.A., "The Pathogenesis and Treatment of Brain Metastases: a Comprehensive Review," C*rit Rev Oncol Hematol*, vol. 52, no. 3, pp. 199-215, 2004.

[36] Traşca D., Şerban A., Ştefanescu V., et. al. "Meningeal Carcinomatosis in a Patient with Crohn's Disease," *Rom. J. Intern. Med*., vol. 52, no. 2, pp. 111-120, 2014.

[37] Wang X., Xu M., Liang H., Xu L., "Comparison of CT and MRI in Diagnosis of Cerebrospinal Leak induced by Multiple Fractures of Skull Base," *Radiol. Oncol*., vol. 45, no. 2, pp. 91-96, 2011.

[38] Yousem D.M., Patrone P.M., Grossman R.I., "Leptomeningeal Metastases: MR Evaluation," *J Comput. Assist. Tomogr*. vol. 14, no. 2, pp. 255-261, 1990.

Mehmet Gül was graduated from Computer Education and Instructional Technology in Middle East Technical University, Ankara, Turkey in 2006. He received master degrees in Computer Engineering in Fırat University, Elazığ, Turkey in 2010. He is PhD student in biomedical Engineering in Fatih University, Istanbul. He studies at image process methods. He has been a computer instructor in Dicle University, Diyarbakır, Turkey since 2009.

Sadık Kara was graduated from Department of Electronics Engineering at Erciyes University in 1988. He had work experiences at various companies such as Turkish Electricity Association, BirlikMensucat Textile Factory, and Military 2nd Maintenance Centre as an engineer. His academic career was started at Erciyes University in 1991 as a Teaching and Research Assistant. In 2000, he received his Assoc. Prof. Degree on Bio-electronics.He had worked in Turkish Journal of Electrical Engineering and Computer Sciences as an Editor in Chief from 2009 to 2014 and has been working as a Professor at Fatih University as well as theHead of Research Project Management Office, Director of the Institute of Biomedical Engineering and Head of Conservatory since 2008. His general research interests include bioinstrumentation, biosignal and image processing, and neural network applications in medicine.

Abdurrahman Işıkdoğan was graduated from faculty of medicine in Dicle University, Diyarbakır, Turkey, in 1991. He received associated professor in medical oncology in Dicle University, in 2004. He has been professor in medical oncology department in Dicle University, Turkey since 2009.

Yusuf Yarar graduated from faculty of medicine, Ege University, İzmir, Turkey. He received radiologist specialist in Adana Numune education and research hospital. He has worked in Selahaddin'iEyyubi State hospital since 2012.